

MANUFACTURING THINNED FRICTION-STIR WELDED 1050 ALUMINUM BY POST ROLLING: MICROSTRUCTURE AND MECHANICAL PROPERTIES

IZDELAVA PLOČEVIN IZ ALUMINIJA 1050 VARJENIH Z GNENENJEM IN NAKNADNIM HLADNIM VALJANJEM; MIKROSTRUKTURA IN MEHANSKE LASTNOSTI

Sina Zinatlou Ajabshir, Mohsen Kazeminezhad*, Amir Hossein Kokabi

Department of Materials Science and Engineering, Sharif University of Technology, Azadi Avenue, Tehran, Iran

Prejem rokopisa – received: 2020-10-19; sprejem za objavo – accepted for publication: 2021-05-26

doi:10.17222/mit.2020.205

One of the friction-stir welding (FSW) limitations is joining thin sheets in sheet-metal manufacturing. To solve this limitation, thicker sheets can be welded with FSW and then rolled to a thinner thickness. This can improve the mechanical properties and save the weld zone soundly. In this work, 3-mm aluminum sheets were joined with FSW. The microstructure and mechanical properties of the samples were assessed at various rotational speeds (ω) and travel speeds (v). Then, the welded samples were cold worked (CW) by rolling them at different percentages so that the samples were 2 mm and 1 mm thick. The effects of welding and post rolling on the mechanical properties and a failure analysis were deliberated. It was shown that welding reduces the transverse ultimate tensile strength (UTS) of FSWed samples by up to 29 % compared to the UTS of the base metal (BM), while rolling FSWed samples increased the UTS of the cold-worked FSWed samples by up to 94.7 % in comparison to the UTS of FSWed samples. Also, during the tensile test of the specimens FSWed at a lower travel speed, a fracture occurred at the stir zone (SZ)/thermo-mechanically affected zone (TMAZ) interface, on the advancing part; however, at a higher travel speed, it occurred at the interface of the heat-affected zone (HAZ) and TMAZ, on the retreating part. Moreover, during the tensile test of the cold-worked FSWed samples, the failure took place at the HAZ and the interface of the SZ and TMAZ, respectively. The UTS was risen by increasing the cold work. The UTS of a specimen FSWed at 50 mm/min and 1200 min⁻¹ went up from 76 MPa to 124 MPa due to 33-% cold work and to 148 MPa due to 66-% cold work; meanwhile, the fracture occurred at the SZ/TMAZ interface or TMAZ of most of the post-rolled FSWed samples.

Keywords: aluminum, friction-stir welding, microstructure, mechanical properties, cold work, post rolling

Ena od glavnih omejitev rotacijskega varjenja z gnetenjem (FSW; angl.: friction stir welding) je povezovanje tankih pločevin med njihovo proizvodnjo. Rešitev tega problema bi bilo varjenje z gnetenjem debelejših pločevin in nato njihovo tanjšanje na želeno debelino. To lahko izboljša mehanske lastnosti pločevin in ohrani celovitost zavarjenega spoja. V članku je opisano raziskovalno-eksperimentalno delo spajanja Al pločevin debeline 3 mm s pomočjo varjenja z gnetenjem. Avtorji so ocenili mikrostrukturo nastalo pri različnih hitrostih vrtenja (ω) in potovanja orodja (v). Nato so varjene vzorce hladno deformirali (CW; angl.: cold worked) z valjanjem pri različnih stopnjah deformacije na debelino pločevin 2 mm in 1 mm. Potem so ocenili vpliv varjenja in naknadnega valjanja na mehanske lastnosti in izdelali analizo poškodb. Ugotovili so, da varjenje z gnetenjem zmanjša prečno natezno porušitveno trdnost vzorcev (UTS) za do 29 % v primerjavi z UTS osnovnega materiala (BM; angl.: base metal). Naknadno hladno valjanje varjenih vzorcev je povečalo UTS za do 94,7 % v primerjavi z UTS samo varjenih vzorcev. Prav tako je med nateznimi preizkusi večine vzorcev, ki so bili varjeni z nižjo hitrostjo potovanja orodja, prihajalo do njihove porušitve na meji prehodne cone in cone mešanja (SZ; angl.: stirring zone). Pri višjih hitrostih potovanja orodja pa je prišlo do porušitve naknadno obdelanih vzorcev na meji med toplotno vplivano cono (HAZ; angl.: heat-affected zone) in termo-mehansko vplivano cono (TMAZ; angl.: thermo mechanical affected zone). Poleg tega je med nateznimi preizkusi FSW in hladno deformiranih vzorcev prihajalo do njihovih porušitev pri HAZ ter na meji med SZ in TMAZ. Natezna trdnost vzorcev se je povečevala s povečevanjem stopnje deformacije. UTS vzorcev, varjenih s hitrostjo potovanja orodja 50 mm/min in hitrostjo vrtenja orodja 1200 min⁻¹, je narasla s 76 MPa na 124 MPa pri 33 % hladni deformaciji in na 148 MPa pri 66 % hladni deformaciji. Pri večini naknadno valjanih vzorcev varjenih z gnetenjem je prelom nastopil na meji SZ/TMAZ ali TMAZ.

Ključne besede: aluminij, rotacijsko varjenje z gnetenjem, mikrostruktura, mehanske lastnosti, hladna deformacija, naknadno valjanje

1 INTRODUCTION

Friction-stir welding (FSW) is one of the joining processes utilized for the materials that are not easily joined with conventional fusion welding methods such as aluminum, and it is widely implemented in some critical applications such as the automotive, aircraft and shipbuilding industries.¹⁻⁷

In general, most of the FSW literature describes the joining of thick sheets. However, Scialpi et al.⁸ studied mechanical properties of micro friction stir welded thin aluminum alloy 6082-T6/2024-T3 sheets (0.8 mm thickness). They reported excellent mechanical properties. But this method (micro friction stir welding) that they studied has some limitations. Firstly, it is not economical as it needs a special tool to deal with thickness. Secondly, the optimization of welding parameters due to the extreme heat transfer of thin sheets and tool geometries

*Corresponding author's e-mail:
mkazemi@sharif.edu

previously mentioned is too time-consuming and meticulous (due to the lack of experimental work with various thin-sheet thicknesses). Galvao et al.⁹ also studied the friction-stir welding of very thin aluminum-alloy sheets of 1 mm. Moreover, Forcellese et al.¹⁰ used pinless tools for welding thin sheets, but their method was not comprehensive and applicable to all thin-sheet thicknesses, because, according to their results, it is necessary to control the dimensions of the tools. On the other hand, a proper shoulder diameter should be found for different materials and thicknesses to plan proper joining. Therefore, all the previous studies of joining thin sheets by FSW used different tool geometries and dimensions, making the process very time-consuming and uneconomical and leading to a low production rate. However, welding sheets of higher thicknesses and then applying one of the deformation methods such as cold rolling is more effective for achieving the desired thickness.

When post cold rolling is applied after welding, it has some advantages. Previous studies showed that mechanical properties, such as the UTS of FSWed samples, are weaker than those of the base metal (BM).^{11,12} So, after post rolling, due to strain hardening, mechanical properties, such as the UTS of FSWed samples, are increased.¹³ Another effect of post rolling is the surface improvement of the weld zone formed by the tool shoulder side.¹⁴

Thus, for joining thin sheets, first, the sheets with a high thickness (> 3 mm) can be joined with FSW and then the thickness of welded samples is decreased by post cold rolling.

By focusing on FSWed sheets that can be thinned by rolling, recently a group of researchers^{15,16} considered post rolling parallel to the welding direction. However, it seems that by exploiting the metal-forming principles, the welding zone is not under any seriously challenging state when the rolling direction is the same as the welding direction. To this end, in the present work, the rolling was performed perpendicularly to the welding direction to evaluate severe conditions in the welding zone.

It is interesting to know the microstructure and mechanical-property evolutions at different zones of FSWed samples during post cold rolling.

Here, 3-mm AA1050 sheets were used as the BM. Wrought sheets were joined with FSW at different rotational speeds and travel speeds (different welding conditions). The mechanical-test and metallographic-analysis results for the joined samples were assessed. The FSWed samples were then cold worked by rolling them along the transverse direction (TD) of welding at different reductions. The evolutions of the microstructure in the SZ and other zones during post rolling were studied. Based on microstructure observations, the influences of post rolling on the mechanical properties and the fracture behavior were described.

2 EXPERIMENTAL WORK

The as-received AA1050 sheet with a chemical composition of 0.62 w/% Fe, 0.51 w/% Si (weight percent) and balanced Al, with dimensions of (150 × 55 × 3) mm, was used. The welding tool, made of simple cylindrical H13 steel, was used, creating a heat-treatment process to obtain a hardness of 54 HRC. The tool dimensions such as shoulder and pin were 12.5 mm and 3 mm in diameter, respectively, and its height was 2.7 mm. The inclination angle was set to 2.5° from the vertical axis in the weld. The FSW conditions – rotation speed, ω , and travel speed, v – were changed from 900 min⁻¹ to 1200 min⁻¹ and 50 mm/min to 150 mm/min, respectively. The samples were fixed during the FSW process. Before the welding, the sheets were prepared with grating paper and washed with acetone. After joining the sheets with FSW, the rolling process was carried out on some joints at room temperature, in the TD of the FSWed samples, as illustrated in **Figure 1a**. The rolling was performed at two different levels of cold work, 33 % (termed as 33 %-cold worked FSWed) and 66 % (termed as 66 %-cold-worked FSWed). For investigating the mechanical properties of the FSWed samples, a transverse

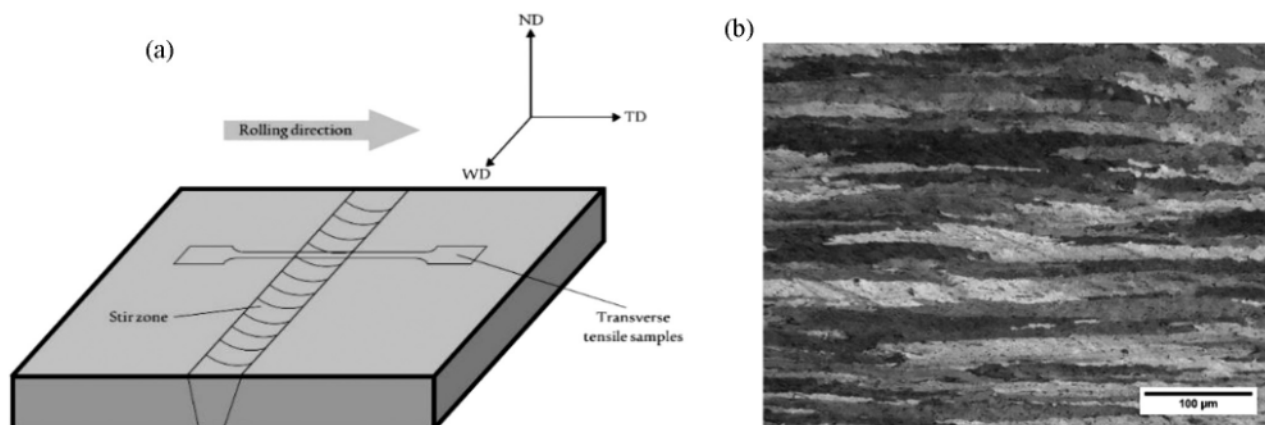


Figure 1: a) Schematic presentation of post cold rolling (transverse direction (TD), welding direction (WD) and normal direction (ND)), b) as-received BM microstructure of AA1050 with the virgin rolled microstructure

tensile test was carried out based on the ASTM-E8M standard, in which the position of the stir zone was in the middle of the gauge length and the microhardness profile was measured. A load of 100 g for 15 s was utilized to measure the Vickers microhardness at the centerline of the cross-section of the samples. The microstructure was studied after polishing and electro etching with HBF_4 2.5 %. The metallographic analysis of different zones of the FSWed samples was carried out using optical microscopy (OM).

3 RESULTS AND DISCUSSION

3.1 Microstructure of FSWed samples

3.1.1 Stir zone

The welded samples obtained at different FSW conditions were observed to find where at the welded zone the cracks and porosity were not visible. In order to have a clear view of the as-received BM, its microstructure is shown in **Figure 1b**. In addition, the microstructures of the SZ of the FSWed samples at different welding parameters are presented in **Figures 2a to 2d**. In all FSW conditions, the microstructures show fine equiaxed grains in the SZ, as confirmed by other researchers.^{11,17–20} This happens due to the continuous dynamic recrystallization that is a result of simultaneous effects of the plastic strain applied to the material in the stir zone and the temperature rise due to the friction between the tool

and specimen during welding.^{21,22} The average size of the SZ grains was measured in accordance with ASTM E112 and the results are shown in **Table 1**.

An increase in the rotational speed increases the average size of the SZ grains at a specific travel speed, as can be seen in **Figure 2** and **Table 1**. The heat input is greater at a higher rotational speed. Therefore, the grains are grown after recrystallization. At a higher travel speed, the heat input is lower in accordance with the relation between ω/v and heat input. Thus, decreasing the travel speed leads to an increase in the grain size of the SZ, which is clearly seen in **Figures 2a to 2d** and **Table 1**. As presented in **Figure 2**, the grain size is in a range of 3.4–5.4 μm while the minimum and maximum grain sizes characterize the samples with the lowest and highest ω/v , respectively. Similar outputs were obtained through FSW of aluminum alloys during other works.^{12,23–25}

3.1.2 Thermo-mechanically affected and heat-affected zones

Microstructures of other welding zones in diverse welding conditions are shown in **Figure 3**. The average sizes of these zone grains are similar to the SZ ones. In the samples with a low travel speed, the maximum heat causes high temperatures and increases the extent of the HAZ and TMAZ. So, this can lead to a grain growth in the HAZ and a slight growth in the TMAZ. The average

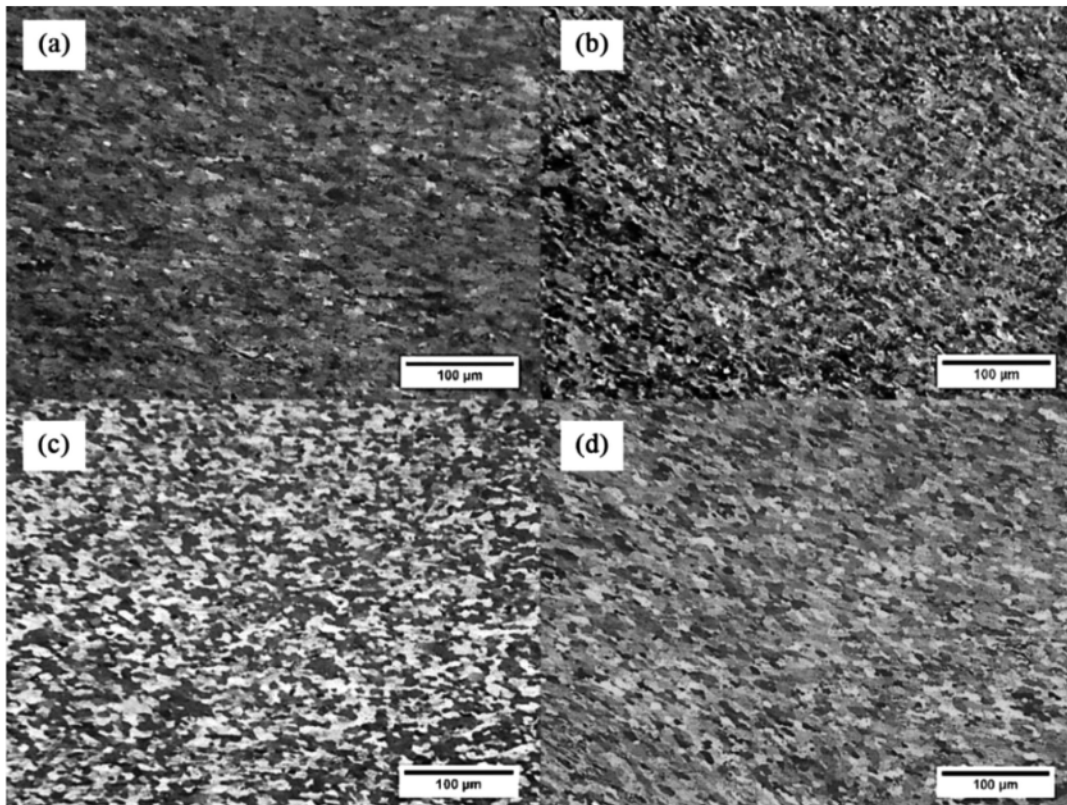


Figure 2: Metallographic analysis of SZ in various welding conditions: a) 900 min^{-1} and 50 mm/min, b) 900 min^{-1} and 150 mm/min, c) 1200 min^{-1} and 50 mm/min, d) 1200 min^{-1} and 150 mm/min

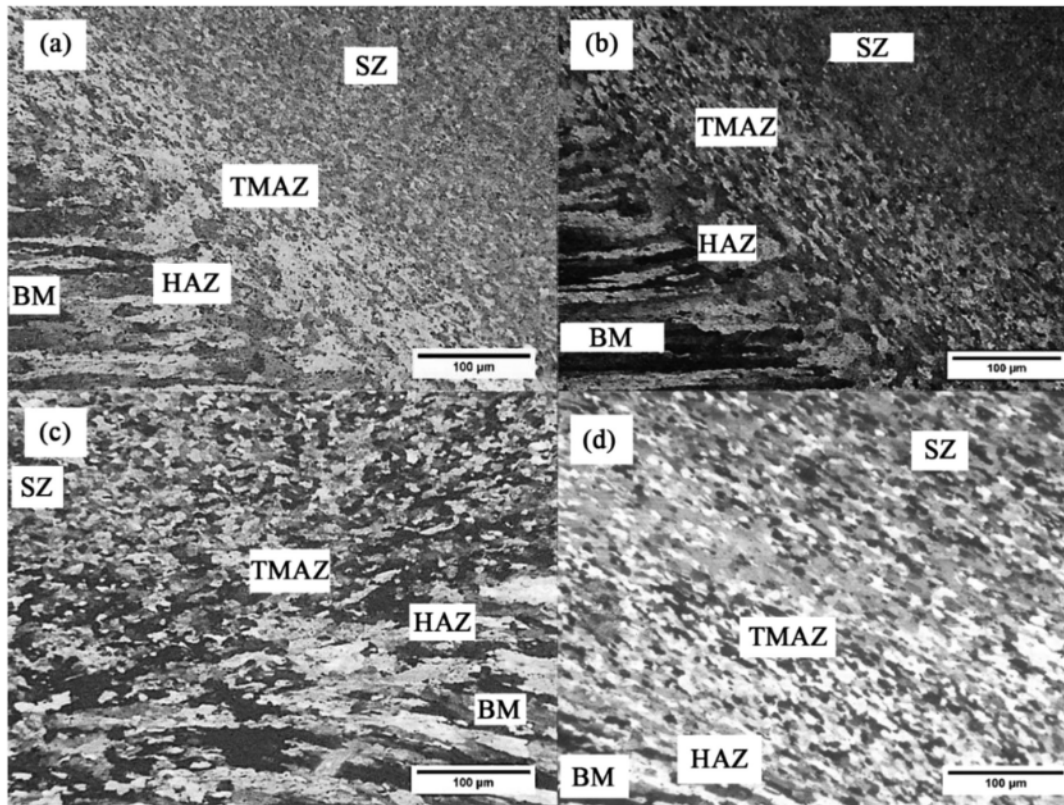


Figure 3: Metallographic analysis of various zones in different welding conditions: a) 900 min⁻¹ and 50 mm/m, b) 900 min⁻¹ and 150 mm/min, c) 1200 min⁻¹ and 50 mm/min, d) 1200 min⁻¹ and 150 mm/min

grain sizes of the HAZ and TMAZ shown in Table 1 affirm this finding and the HAZ range is from 9.1–11.1 μm and the TMAZ range is from 8.3–9.1 μm. Similar outcomes were reported for aluminum sheets joined with FSW in other works.^{12,20}

3.2 Microstructures of cold-worked FSWed samples

To understand the changes in the SZ microstructures during the rolling process, the microstructures of the 33 % cold-worked FSWed sample and 66 % cold-worked FSWed sample were studied with OM, and the results are included in Figure 4. According to Figures 4a to 4h, the SZ fine equiaxed grains are elongated in the rolling direction. After rolling, there is no interruption or dissociation in the weld zone (WZ) or the WZ/BM interface. The levels of grain elongation are different, depending on the level of cold work; so, the aspect ratio (AR) can be defined in this research. The AR is the ratio of the grain size in the rolling direction to the width of grains. The ARs of the SZs obtained at different cold-working percentages (CW %) are given in Table 1. According to Figure 4 and Table 1, when the CW % is increased, the AR is increased and the grain sizes are decreased. In Figures 5a to 5h, a remarkable point is tilting of the grain-boundary orientation with the HAZ rolling direc-

tion and the TMAZ/SZ interface. After post rolling, the tilting of the grain-boundary orientation with the rolling direction is decreased, which leads to an increase in the TMAZ mechanical strength. Since the tilting with the rolling direction in the TMAZ is higher, a fracture in that zone can be seen later. In summary, due to the increase in the CW %, the AR is increased and it has a positive influence on the mechanical properties.

Table 1: Average grain size of FSWed weld zones and the AR of the stir zones of cold-worked FSWed samples at various welding parameters and different CW % levels

ω (min ⁻¹)	v (mm/min)	CW (%)	Average grain size (μm)			AR
			SZ	TMAZ	HAZ	
900	50	0	4.0	8.6	9.8	–
		33	–	–	–	2.18
		66	–	–	–	4.86
	150	0	3.4	8.3	9.1	–
		33	–	–	–	2.77
		66	–	–	–	9.86
1200	50	0	5.4	9.1	11.1	–
		33	–	–	–	2.26
		66	–	–	–	4.53
	150	0	4.2	8.9	10.3	–
		33	–	–	–	2.66
		66	–	–	–	9.53

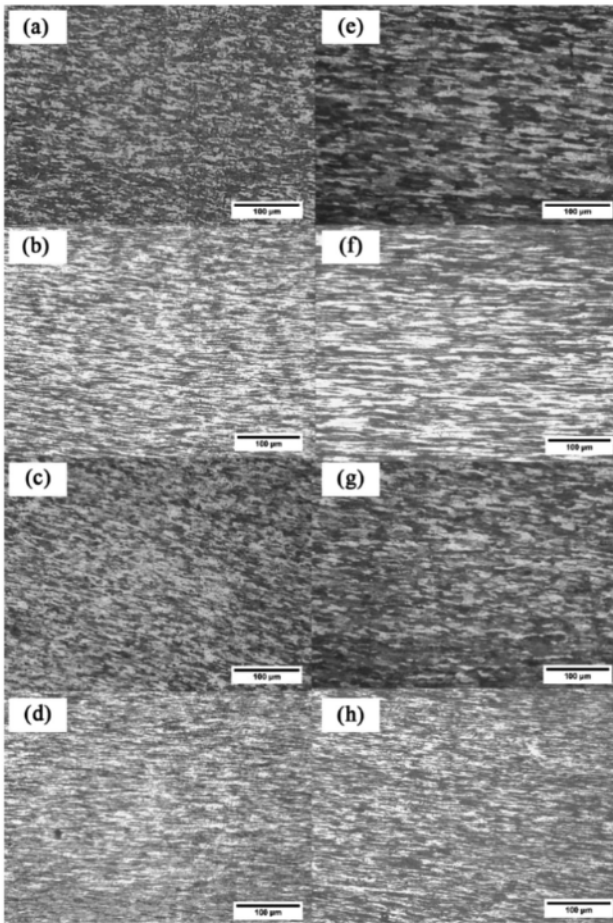


Figure 4: Metallographic analysis of the stir zones of cold-worked FSWed samples at various welding conditions and different CW % levels: a) 900 min^{-1} , 50 mm/min, 33 %; b) 900 min^{-1} , 50 mm/min, 66 %; c) 900 min^{-1} , 150 mm/min, 33 %; d) 900 min^{-1} , 150 mm/min, 66 %; e) 1200 min^{-1} , 50 mm/min, 33 %; f) 1200 min^{-1} , 50 mm/min, 66 %; g) 1200 min^{-1} , 150 mm/min, 33 %; h) 1200 min^{-1} , 150 mm/min, 66 %

3.3 Mechanical properties

3.3.1 Mechanical properties of FSWed samples

The mechanical properties of the virgin BM, including UTS, hardness and elongation, are 102 MPa, 44 HV, and 31 %, respectively, while the tensile properties of the as-received sheet sample are much higher than those of the FSWed samples. Similar results can be found in some prior researches.^{12,20} Table 2 presents the yield stress (YS) and UTS of the FSWed samples under different welding parameters where the welding parameters have various effects on the YS and UTS of the FSWed samples. A rotational-speed increase or travel-speed decrease cause a reduction in the YS and UTS of the FSWed samples. This reduction is due to the heat input imposed on the specimens, leading to a grain growth in the SZ (Figure 2 and Table 1). Similar results were reported by Amiri et al.¹¹ The range of the FSWed sample UTS at various welding parameters is 76–80 MPa. Another important mechanical property is the elongation.

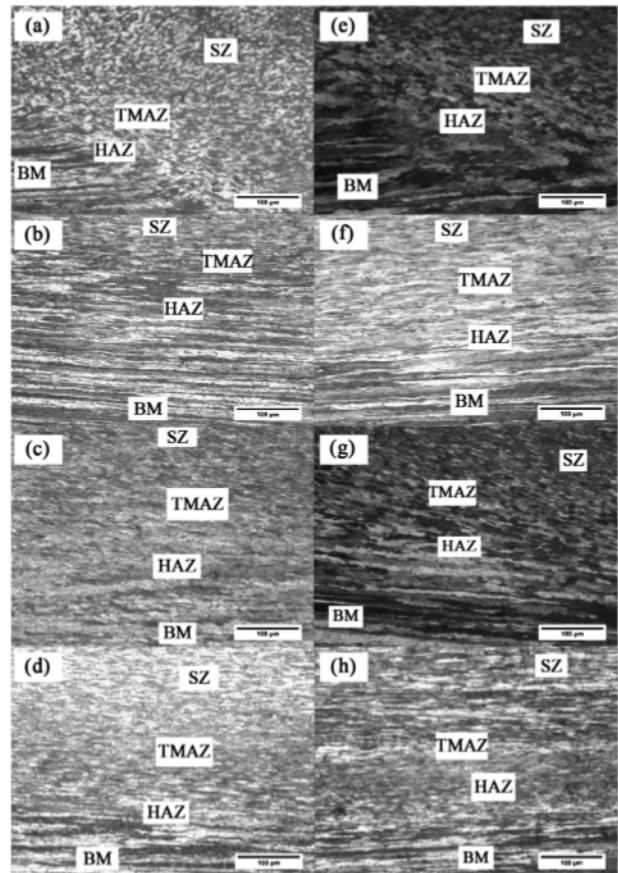


Figure 5: Metallographic analysis of different zones of cold-worked FSWed samples at various welding conditions and different CW % levels: a) 900 min^{-1} , 50 mm/min, 33 %; b) 900 min^{-1} , 50 mm/min, 66 %; c) 900 min, 150 mm/min, 33 %; d) 900 min^{-1} , 150 mm/min, 66 %; e) 1200 min^{-1} , 50 mm/min, 33 %; f) 1200 min^{-1} , 50 mm/min, 66 %; g) 1200 min^{-1} , 150 mm/min, 33 %; h) 1200 min^{-1} , 150 mm/min, 66 %

According to Table 2, the minimum travel speed leads to the maximum heat generation and, consequently, the risen temperature increases the elongation.^{12,24,26} Elongation values at various travel speeds are listed in Table 2. The range of the elongation of the FSWed samples is 7.13–14.38 %.

The welding heat input affects the microstructure and mechanical properties of different welding zones. Heat input leads to metallurgical changes, such as grain growth and softening, which results in a hardness decrease. Usually, the fracture of FSWed samples through a tensile test starts at the zone with the minimum hardness.^{12,24,26} Generally, changes in the welding parameters lead to different amounts of heat input. For example, a low travel speed leads to an increase in the heat input and a high heat input makes the softening zone susceptible to fracture. So, since here the BM is in the as-received state and the SZ has fine equiaxed grains, the tilt of the orientation of grain boundaries with the tensile direction and TMAZ elongated grains causes a fracture at the TMAZ/SZ interface. Similar results were obtained by Sarkari Khorami et al.²⁷

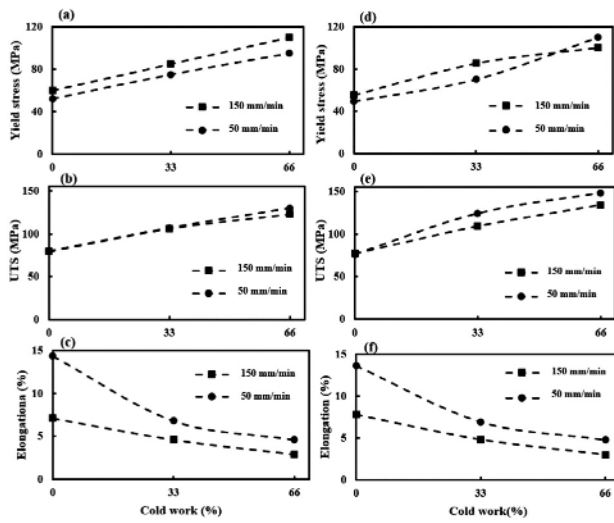


Figure 6: Mechanical properties of cold-worked FSWed samples at various welding conditions and different CW % for $\omega = 900 \text{ min}^{-1}$: a) yield stress, b) UTS, c) elongation, and for $\omega = 1200 \text{ min}^{-1}$: d) yield stress, e) UTS, f) elongation

During the tensile test, the fracture occurs at the TMAZ/SZ interface (Figures 7a and 7g) and HAZ/TMAZ interface (Figures 7b and 7h) at low and high travel speed, respectively. The failing side that follows the welding parameters is another noticeable thing in the mechanical behavior of the joining. The fracture part is located on the advancing side (AS) and the retreating side (RS) for the low and high travel speed, respectively. Similar results were reported in other researches.¹² In the HAZ and TMAZ, a low travel speed and the same direction of travel and rotational speed of the FSW tool on the AS that generated the high heat input^{2,12,25} leading to the grain growth and thermal softening, higher than that on the RS, corresponds to the location of the fracture on the AS. On the contrary, for a higher travel speed, the fracture is at the TMAZ/HAZ interface on the RS due to the heat generated from plastic strain.^{2,12,25} All the mechani-

cal properties of the FSWed samples are given in Table 2.

The average hardness of each zone extracted from the hardness profiles of the cross-sections of the FSWed samples are seen in Figures 8a and 8b. As can be seen, the hardness of the SZ for all welding parameters is lower than that of the BM.^{20,25,27} This reduction in the hardness after welding is due to the wrought microstructure of the as-received state of the BM and grain growth due to heat input. According to Figure 8, for the FSWed samples (0 % CW) with a low travel speed, it can be considered that the maximum heat generation causes a higher temperature and augments the extent of the HAZ. Also, this can be related to the slight grain growth in the SZ that can decrease the hardness in this zone. Other researches showed similar results relating to this issue.^{22,25} According to Figure 8, at the low travel speed (high heat input), recrystallization may occur at the HAZ that leads to an increase in the hardness.²⁵ Also, the hardness level for the FSWed samples at all the zones are decreased on Figure 8b compared to those from Figure 8a, which may be due to the increased rotational speed and, consequently, increased heat input.

3.3.2 Mechanical properties of cold-worked FSWed samples

After post rolling, the transverse tensile properties notably increased. Generally, the strength of the FSWed samples can be influenced by the dislocation density, grain size and reduction in the tilt of the grain-boundary orientation with the tensile direction at the SZ/TMAZ interface after post rolling. Figure 6 shows the YS and UTS of the cold-worked FSWed samples. With increasing CW % and, consequently, increasing dislocation density due to exploiting the fundamentals of work hardening and grain strengthening,^{28,29} the YS and UTS are increased (Figure 6). The UTS of the cold-worked FSWed samples increased from 32.4 % to 94.7 % compared to the FSWed samples. The range of the cold-

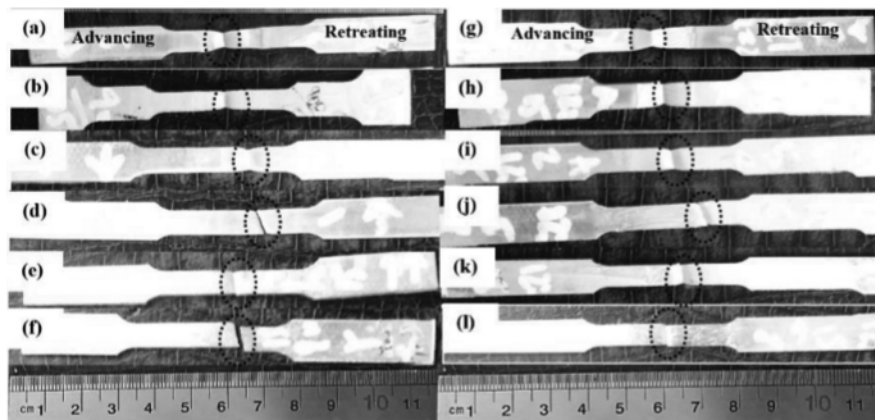


Figure 7: Failure locations on FSWed and cold-worked FSWed samples exposed to transverse tensile tests at different welding conditions and different CW %: a) 900 min⁻¹, 50 mm/min, b) 900 min⁻¹, 150 mm/min, c) 900 min⁻¹, 50 mm/min, 33 %, d) 900 min⁻¹, 50 mm/min, 66 %, e) 900 min⁻¹, 150 mm/min, 33 %, f) 900 min⁻¹, 150 mm/min, 66 %, g) 1200 min⁻¹, 50 mm/min, h) 1200 min⁻¹, 150 mm/min, i) 1200 min⁻¹, 50 mm/min, 33%, j) 1200 min⁻¹, 50 mm/min, 66 %, k) 1200 min⁻¹, 150 mm/min, 33 %, l) 1200 min⁻¹, 150 mm/min, 66 %

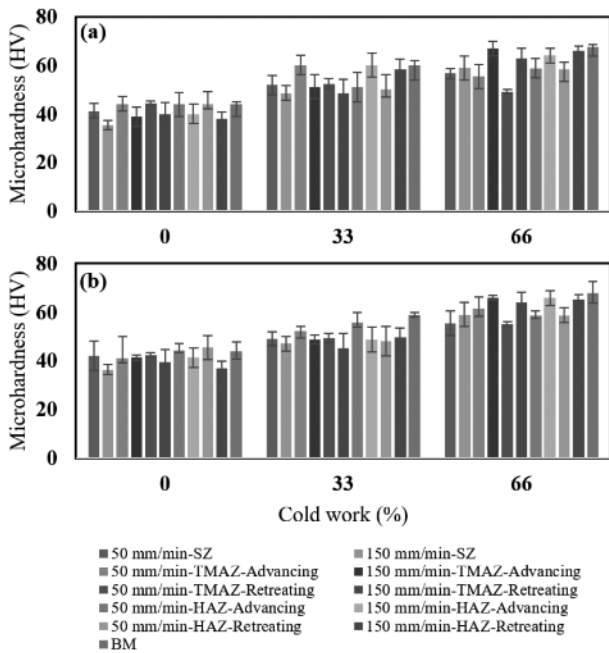


Figure 8: Average hardness of each zone at the cross-sections of the samples: a) 900 min⁻¹, b) 1200 min⁻¹

worked FSWed sample UTS is 106–148 MPa at various welding parameters and different CW %. In general, as can be seen on Figures 6c and 6f, the elongation of the cold-worked FSWed samples decreased compared with the FSWed samples due to increased work hardening.

The fracture location of the cold-worked FSWed samples follows the changes in the heat input, grain size and tilt of the orientation of grain boundaries with the tensile direction at the SZ/TMAZ interface after post rolling. The zones of the cold-worked FSWed samples exhibit just a small tilt of the orientation of grain boundaries with the tensile direction at the TMAZ/SZ interface and TMAZ. Also, it is obvious that fracture does not take place at the BM because it has a wrought microstructure; neither does it occur at the SZ because the SZ has more wrought fine grains than the other welding zones after

post rolling. Furthermore, the tilt of the orientation of grain boundaries with the tensile direction decreases the mechanical properties of these zones. As it is expected, fracture takes place at these zones. However, for some cold-worked FSWed samples that are welded at a low travel speed (high heat input), fracture occurs at the wrought coarse-grained HAZ because the HAZ is softened during welding and this zone may be the necking start point.

Figure 7 shows fracture locations on the cold-worked FSWed samples. In general, the fracture location on most cold-worked FSWed samples is at the retreating side (RS). As the stored strain energy at the RS is high during welding, after post rolling, the strain hardening is increased and for this reason, the fracture takes place at the RS. All the mechanical properties of the post-rolled FSWed samples are shown in Table 2. Figures 8a and 8b show the average hardness of the weld zones after post rolling obtained from the hardness profiles of the cross-sections of the cold-worked FSWed samples. According to the visual test in this work, it is observed that with the increasing CW %, the extent of the SZ is dramatically increased. So, with the CW % increased from 33 % to 66 %, the SZ width is almost stretched. In general, the hardness of the cold-worked FSWed samples is strongly increased due to strain hardening, increased dislocation density and reduced grain size.^{28–30}

4 CONCLUSIONS

In this work, remarkable results were obtained, resolving the FSW problem about thin-sheet joining. The concluded points are:

1. After post rolling, there is no interruption or dissociation at the weld zone (WZ) and WZ/BM interface. So, to decrease the thickness of welded sheets and obtain the critical thickness, we can use post cold work as it has positive effects on mechanical properties.

2. In general, microhardness distribution at the cross-sections of all the FSWed and cold-worked FSWed

Table 2: Mechanical properties of cold-worked FSWed samples

ω (min ⁻¹)	v (mm/min)	CW (%)	UTS (MPa)	YS (MPa)	Reduction of BM UTS (%)	Enhancement of BM UTS (%)	Enhancement of UTS with FSW (%)	Elongation (%)	Fracture location
900	50	0	80	52	21.5	–	–	14.38	SZ/TMAZ
		33	107	75	–	4.9	33.7	6.81	HAZ
		66	130	95	–	27.4	62.5	4.6	TMAZ
	150	0	79	60	22.5	–	–	7.13	TMAZ/HAZ
		33	106	85	–	3.9	32.4	4.6	SZ/TMAZ
		66	123	110	–	20.5	55.7	2.9	TMAZ
1200	50	0	76	49	25.4	–	–	13.6	SZ/TMAZ
		33	124	70	–	21.5	63.1	6.94	HAZ
		66	148	95	–	45	94.7	4.8	TMAZ
	150	0	77	55	24.5	–	–	7.8	TMAZ/HAZ
		33	109	85	–	6.8	43.4	4.81	TMAZ
		66	134	100	–	31.3	76.3	3	SZ/TMAZ

samples clearly confirms the existence of the observed microstructure.

3. Welding caused a UTS reduction for the FSWed samples of up to 29 % compared to the UTS of the BM. On the other hand, after post rolling, the UTS of the cold-worked FSWed samples increased by up to 94.7 % compared to the UTS of the FSWed samples.

4. The highest UTS is related to the FSWed sample cold-worked at a 50 mm/min travel speed, 1200 r/min rotational speed and 66 CW %. The UTS of this sample is 148 MPa, which is by 45 % and 94.7 % higher than those of the BM and FSWed samples, respectively.

5. The fracture locations of the FSWed samples are significantly dependent on the parameters that change during the welding. So, the fracture occurs at the TMAZ/SZ interface, on the AS at 50 mm/min, and at the HAZ/TMAZ interface, on the RS at 150 mm/min.

6. The fracture locations of most cold-worked FSWed samples are strongly dependent on the tilt of the orientation of grain boundaries with the tensile direction, so they occur at the TMAZ and TMAZ/SZ interface, on the RS.

Acknowledgments

The authors thank the research board of the Sharif University of Technology, Iran, for the provision of research facilities used for this work.

5 REFERENCES

- W. M. Thomas, Friction Stir Welding of Ferrous Materials; A Feasibility Study, *Sci. Technol. Weld. Join.*, 4 (1999) 1, 1–11, doi:10.1179/136217199101538012
- R. S. Mishra, Z. Y. Ma, Friction stir welding and processing, *Mater. Sci. Eng. R: Reports*, 50 (2005) 1–2, 1–78, doi:10.1016/j.mser.2005.07.001
- W. Thomas, E. Nicholas, Friction stir welding for the transportation industries, *Mater. Des.*, 18 (1997) 4–6, 269–273, doi:10.1016/S0261-3069(97)00062-9
- J. H. Cho, D. E. Boyce, P. R. Dawson, Modeling strain hardening and texture evolution in friction stir welding of stainless steel, *Mater. Sci. Eng. A-Structural Mater. Prop. Microstruct. Process.*, 398 (2005) 1–2, 146–163
- Y.-M. Hwang, Z.-W. Kang, Y.-C. Chiou, H.-H. Hsu, Experimental study on temperature distributions within the workpiece during friction stir welding of aluminum alloys, *Int. J. Mach. Tools Manuf.*, 48 (2008) 7–8, 778–787, doi:10.1016/j.ijmactools.2007.12.003
- C. Zhou, X. Yang, G. Luan, Investigation of microstructures and fatigue properties of friction stir welded Al-Mg alloy, *Mater. Chem. Phys.*, 98 (2006) 2–3, 285–290, doi:10.1016/j.matchemphys.2005.09.019
- R. Nandan, T. Debroy, H. K. D. H. Bhadeshia, Recent advances in friction-stir welding – Process, weldment structure and properties, *Prog. Mater. Sci.*, (2008), doi:10.1016/j.pmatsci.2008.05.001
- A. Scialpi, M. De Giorgi, L. A. C. De Filippis, R. Nobile, F. W. Panella, Mechanical analysis of ultra-thin friction stir welding joined sheets with dissimilar and similar materials, *Mater. Des.*, 29 (2008) 5, 928–936, doi:10.1016/j.matdes.2007.04.006
- D. R. Ivan Galvao, Carlos Leitao, Altino Loureiro, Friction Stir Welding of Very Thin Plates, *Soldag. Insp. Sao Paulo*, 17 (2012), 2–10, doi:10.1590/S0104-92242012000100002
- A. Forcellese, F. Gabrielli, M. Simoncini, Mechanical properties and microstructure of joints in AZ31 thin sheets obtained by friction stir welding using “pin” and “pinless” tool configurations, *Mater. Des.*, 34 (2012), 219–229, doi:10.1016/j.matdes.2011.08.001
- M. Amiri, M. Kazeminezhad, A. H. Kokabi, Energy absorption of friction stir welded 1050 aluminum sheets through wedge tearing, *Mater. Des.*, 93 (2016), 216–223, doi:10.1016/j.matdes.2015.12.163
- B. Abnar, M. Kazeminezhad, A. H. Kokabi, Effects of heat input in friction stir welding on microstructure and mechanical properties of AA3003-H18 plates, *Trans. Nonferrous Met. Soc. China*, 25 (2015) 7, 2147–2155, doi:10.1016/S1003-6326(15)63826-2
- R. Xin, D. Liu, Z. Xu, B. Li, Q. Liu, Changes in texture and microstructure of friction stir welded Mg alloy during post-rolling and their effects on mechanical properties, *Mater. Sci. Eng. A*, 582 (2013), 178–187, doi:10.1016/j.msea.2013.06.005
- F. Gabrielli, A. Forcellese, M. El Mehtedi, M. Simoncini, Mechanical Properties and Formability of Cold Rolled Friction Stir Welded Sheets in AA5754 for Automotive Applications, *Procedia Eng.*, 183 (2017), 245–250, doi:10.1016/j.proeng.2017.04.030
- N. F. M. Selamat, A. H. Baghdadi, Z. Sajuri, S. Junaidi, A. H. Kokabi, Rolling effect on dissimilar friction stir welded AA5083-AA6061 aluminium alloy joints, *J. Adv. Manuf. Technol.*, 14 (2020)
- Z. Sajuri, N. F. M. Selamat, A. H. Baghdadi, A. Rajabi, M. Z. Omar, A. H. Kokabi, J. Syarif, Cold-rolling strain hardening effect on the microstructure, serration-flow behaviour and dislocation density of friction stir welded AA5083, *Metals (Basel)*, 10 (2020) 1, doi:10.3390/met10010070
- Y. S. Sato, Y. Kurihara, S. H. C. Park, H. Kokawa, N. Tsuji, Friction stir welding of ultrafine grained Al alloy 1100 produced by accumulative roll-bonding, *Scr. Mater.*, 50 (2004) 1, 57–60, doi:10.1016/j.scriptamat.2003.09.037
- Y. F. Sun, H. Fujii, N. Tsuji, Microstructure and mechanical properties of spot friction stir welded ultrafine grained 1050 Al and conventional grained 6061-T6 Al alloys, *Mater. Sci. Eng. A*, 585 (2013), 17–24, doi:10.1016/j.msea.2013.07.030
- L. E. Murr, G. Liu, J. C. McClure, Dynamic recrystallization in friction-stir welding of aluminium alloy 1100, *J. Mater. Sci. Lett.*, 16 (1997) 22, 1801–1803, doi:10.1023/A:1018556332357
- T. Sakhthivel, G. S. Sengar, J. Mukhopadhyay, Effect of welding speed on microstructure and mechanical properties of friction-stir-welded aluminum, *Int. J. Adv. Manuf. Technol.*, 43 (2009) 5–6, 468–473, doi:10.1007/s00170-008-1727-7
- J.-Q. Su, T. W. Nelson, C. J. Sterling, Microstructure evolution during FSW/FSP of high strength aluminum alloys, *Mater. Sci. Eng. A*, 405 (2005) 1–2, 277–286, doi:10.1016/j.msea.2005.06.009
- Y. Sun, H. Fujii, Y. Takada, N. Tsuji, K. Nakata, K. Nogi, Effect of initial grain size on the joint properties of friction stir welded aluminum, *Mater. Sci. Eng. A*, 527 (2009) 1–2, 317–321, doi:10.1016/j.msea.2009.07.071
- T. Hirata, T. Oguri, H. Hagino, T. Tanaka, S. W. Chung, Y. Takigawa, K. Higashi, Influence of friction stir welding parameters on grain size and formability in 5083 aluminum alloy, *Mater. Sci. Eng. A*, 456 (2007) 1–2, 344–349, doi:10.1016/j.msea.2006.12.079
- C. Sharma, D. K. Dwivedi, P. Kumar, Effect of welding parameters on microstructure and mechanical properties of friction stir welded joints of AA7039 aluminum alloy, *Mater. Des.*, 36 (2012), 379–390, doi:10.1016/j.matdes.2011.10.054
- M. Sarkari Khorami, M. Kazeminezhad, A. H. Kokabi, Microstructure evolutions after friction stir welding of severely deformed aluminum sheets, *Mater. Des.*, 40 (2012), 364–372, doi:10.1016/j.matdes.2012.04.016
- H. Liu, H. Fujii, M. Maeda, K. Nogi, Heterogeneity of mechanical properties of friction stir welded joints of 1050-H24 aluminum alloy, *J. Mater. Sci. Lett.*, 22 (2003) 6, 441–444, doi:10.1023/A:1022959627794

- ²⁷ M. S. Khorami, M. Kazeminezhad, A. H. Kokabi, Mechanical properties of severely plastic deformed aluminum sheets joined by friction stir welding, *Mater. Sci. Eng. A*, 543 (2012), 243–248, doi:10.1016/j.msea.2012.02.082
- ²⁸ D. A. Hughes, N. Hansen, The microstructural origin of work hardening stages, *Acta Mater.*, 148 (2018), 374–383, doi:10.1016/j.actamat.2018.02.002
- ²⁹ T. Narutani, J. Takamura, Grain-size strengthening in terms of dislocation density measured by resistivity, *Acta Metall. Mater.*, 39 (1991) 8, 2037–2049, doi:10.1016/0956-7151(91)90173-X
- ³⁰ M. Milad, N. Zreiba, F. Elhalouani, C. Baradai, The effect of cold work on structure and properties of AISI 304 stainless steel, *J. Mater. Process. Technol.*, 203 (2008) 1–3, 80–85, doi:10.1016/j.jmatprotec.2007.09.080